Phys. Status Solidi C 6, No. 12, 2626–2631 (2009) / DOI 10.1002/pssc.200982555

physica status solidi c
www.pss-c.com
current topics in solid state physics

Structural perfection of InGaN layers and its relation to photoluminescence

Z. Liliental-Weber[1*], K. M. Yu[1], M. Hawkridge[1], S. Bedair[2], A.E. Berman[2], A. Emara[2], D. R. Khanal[1,3], J. Wu[1,3], J. Domagala[4], and J. Bak-Misiuk[4]**

[1] Materials Science Division, Lawrence Berkeley National Laboratory, m/s 62R203-8255, Berkeley, CA 94720, USA
[2] Electrical and Computer Engineering Department, North Carolina State University, Raleigh, NC 27695, USA
[3] Department of Materials Science and Engineering, UC Berkeley, CA 94720, USA
[4] Institute of Physics Polish Academy of Sciences, Al. Lotnikow 32/46, 02-668 Warsaw, Poland

Received 16 June 2009, accepted 6 October 2009
Published online 16 November 2009

PACS 61.05.cp, 61.72.Nn, 61.72.Qq, 68.35.Dv, 68.37.Lp, 78.55.Cr

[*] Corresponding author: e-mail z_liliental-weber@lbl.gov, Phone: +01 510 486 6276, Fax: +01 510 486 4995
[**] e-mail KMYu@lbl.gov, Phone: +01 510 486 6656, Fax: +01 510 486 5530

The relation between structural perfection and optical properties of InGaN with 10% In are discussed. Transmission Electron Microscopy, X-ray diffraction and Rutherford backscattering spectrometry measurements show that only strained layers with a thickness not exceeding 100 nm are defect free and In concentration is lower than the nominal value. Extension of layer thickness leads to layer sequestration into sublayers with different In contents and the formation of planar defects as a result of layer relaxation. In concentration in such sublayers reach and in some cases exceed the nominal concentration. A single band edge photoluminescence peak is observed only for the thinnest layer. Samples with larger film thickness showed multiple PL peaks corresponding to layers with different In content. Much higher In content would be required to explain the presence of some PL peaks, suggesting that some PL peaks originate from the defective areas of the film. This was confirmed by cathodoluminescence studies performed on the same samples used earlier for TEM studies.

© 2009 WILEY-VCH Verlag GmbH & Co. KGaA, Weinheim

1 Introduction InGaN has attracted many researchers as an alloy system with potential applications in light emitting devices and solar cells since by varying In content; one can change the bandgap over a large spectral range [1-3]. Depending on the application, different compositions and different layer thickness need to be used. Due to the miscibility gap in this ternary system that has been theoretically predicted and experimentally observed [4-6], it was believed that layers with In content larger than 20% are difficult to grow. The difficulty of growth of this compound was related to large atomic radii differences between the constituents. Earlier studies of InGaN layers with In content larger that 40% show that such layers can be grown, but some sequestration takes place and two sublayers are formed: strained and relaxed, each with a different In content and different arrangement of structural defects [7-9]. Since different compositions and different layer thicknesses are needed we were interested in how the structural film quality is changing when the layer thickness increases. We chose In contents not larger than 10% since often small In concentrations are used in active areas of optoelectronic devices.

2 Experimental Five $In_xGa_{1-x}N$ samples (x = 0.10) were grown at 800-830 °C by metalorganic chemical vapor deposition (MOCVD) on a 0.5 µm thick layer of GaN grown on Al_2O_3. The samples were expected to have a nominally constant In composition of 10% but increasing film thickness of ~100 nm, 250 nm, 500 nm, 750 nm and 1000 nm. Different experimental techniques including Transmission Electron Microscopy (TEM) in cross-section configuration, X-ray diffraction (XRD) and Rutherford backscattering spectrometry (RBS) were used for structural characterization. Photoluminescence (PL) and cathodoluminescence (CL) studies were carried out in order to correlate the structure of the films with their optical properties.

A JEOL 3010 with 300 keV accelerating voltage and a resolution of 2.4 Å, JEOL CM300 with sub-Angstrom resolution and Philips Tecnai microscope for Z-contrast high resolution studies have been used for detailed struc-

© 2009 WILEY-VCH Verlag GmbH & Co. KGaA, Weinheim

tural characterization. Two thin slabs of samples were cut in two perpendicular orientations, glued together, polished to a thickness of 10 µm and then ion milled until a small perforation occurred to obtain electron transparent samples for TEM studies.

High resolution X-ray diffraction (HRXRD) was used in order to determine the strain, mosaicity and the chemical composition of the ternary alloys from larger areas of the samples by collecting 2θ/ω scans and reciprocal space maps (RSM). HRXRD work was carried out using a Philips X'Pert MRD diffractometer operated with CuKα radiation. The out-of-plane lattice parameter (*c*) was determined using the 0002 reflection in the triple axis geometry. For the in plane lattice parameter (*a*) asymmetric $\underline{11}24$ reflections were collected in glancing-exit geometry with double axis configuration.

The composition and thickness of the InGaN films were also determined by Rutherford backscattering spectrometry (RBS) using a 2 MeV $^{4}He^{+}$ beam at a backscattering angle of 165°. For optimum depth resolution of better than 20 nm, some of the samples were tilted at an angle of 50° with respect to the ion beam. The epitaxial quality of the films was studied by aligning the ion beam with the <0001> axis of the sample.

Cathodoluminescence measurements were performed on a Zeiss Supra SEM with a home-built fiber optic and spectrometer (Ocean Optics) collection system. All measurements were done at room temperature with a 10 kV electron beam.

3 The experimental results

3.1 Photoluminescence (PL) studies Intriguing PL results were obtained on the studied samples. Photoluminesce peak position from the thinnest sample was obtained at 410 nm. This corresponds to an InN fraction of 10% if the PL comes from the band edge luminescence consistent with the expected nominal composition. However with an increase of sample thickness a monotonic increase in the PL peak position from 410 to 455 nm was observed for samples with nominal thickness from 100 to 500 nm (Fig. 1). This would correspond to an increase of InN fraction up to 18% for the band edge luminescence, but this was not expected from the growth. In addition, a second peak at 490 nm started to appear for the sample with 500 nm nominal thickness, corresponding to a film with much higher InN fraction. Further increase in film thickness to 750 nm results in broadening and blue shift of the PL peak. Careful examination reveals that the broad PL peak for this sample consists of three peaks at about 405, 425 and 442 nm. This would again require different InN fractions of 9, 12.5 and 15%, respectively. The multiple peaks also appeared in the thickest sample but their origin was not clear.

Appearance of multiple PL peaks in InGaN is normally attributed to the presence of In droplets [10-13]. With the relatively low In content in our samples droplets are not expected. In addition, there is some dispute on the in-situ occurrence of these droplets due to high-energy electrons used during observation by TEM [14]. Since only the top ~300 nm was sampled by the PL measurement, the difference in the PL results as the film thickness increased reflects the change in the sample perfection with the layer thickness. Since only in InGaN with higher In concentrations has a miscibility gap been predicted [4], the low In concentration (10%) in our sample is not usually considered as problematic. Therefore, we expect that the multiple PL peaks must have a different origin than an increased In content alone. We used different methods to learn about the structural quality of our samples and also used CL on cross-sectional TEM samples to obtain the spectra from different areas of the samples in order to understand the origin of the multiple peaks in PL.

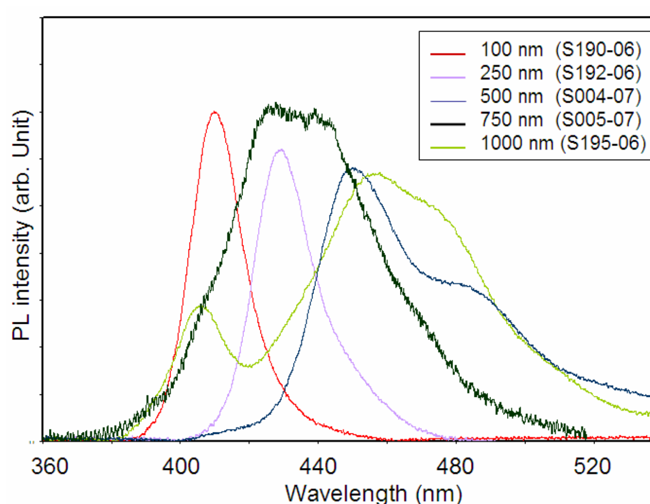

Figure 1 Normalized PL intensities from the studied samples. Nominal sample thickness is indicated.

3.2 TEM studies A thickness measurement by bright field TEM from all five samples in cross-section configuration showed slight differences compared to the nominal thicknesses. Already for the thinnest sample (nominal-100 nm thick), the measured thickness was only 69 nm. We observe that the higher the InGaN layer thickness, the larger the differences between the nominal and observed thickness. The measured thickness for the remaining samples was 200 nm, 400 nm, 520 nm and 730 nm compared to the nominal value of 250 nm, 500 nm, 750 nm and 1000 nm. A TEM image of the thinnest sample (100 nm nominal) (Fig. 2a) shows that this sample was practically defect-free. A small difference in the diffraction contrast allows us to determine the location of the interface (Fig. 2a). Only occasionally could some stacking faults be observed, but not more than 2-3 defects in all transparent areas of the sample (larger than 1 mm in length). The sample surface was very smooth.

© 2009 WILEY-VCH Verlag GmbH & Co. KGaA, Weinheim

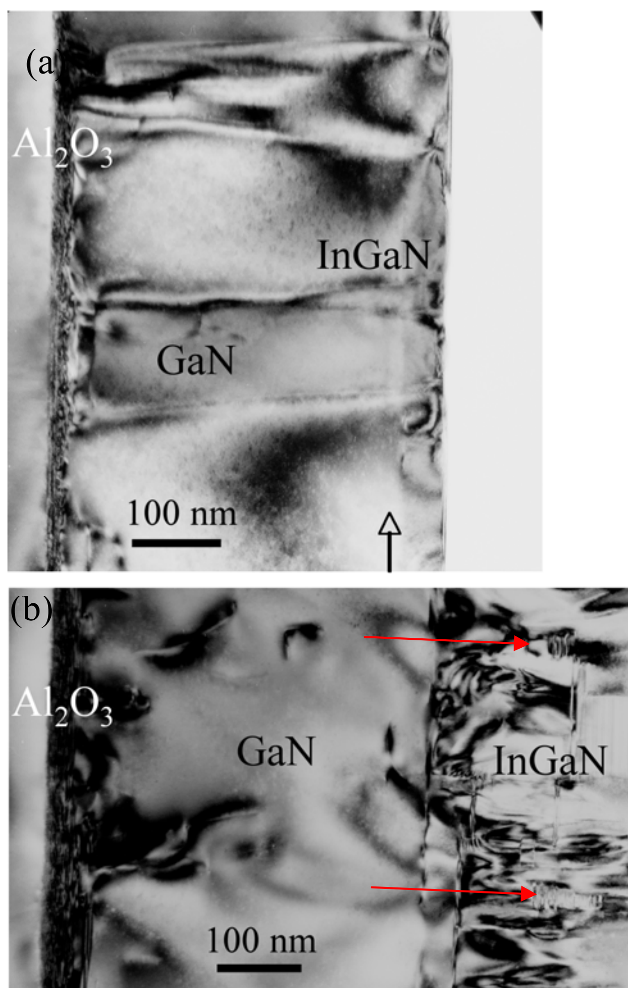

Figure 2 Cross-section TEM micrographs; (a) from the thinnest sample (nominal 100 nm-measured 69 nm). The arrow indicates the interface. Note high structural perfection of this sample; (b) from the thick sample (nominal 750 nm-measured 520 nm). Only part of the sample close to the interface is shown. Note high defect density. Some domains with closely arranged planar defects are indicated by arrows.

With an increase of sample thickness more planar defects could be found located above 70-80 nm from the interface. In most cases they were surrounded by small V-shape voids. Their density also increased and the lateral distance between them was already a few hundred nanometers. The surface of the 200 nm thick sample started to be undulated. Some depressions could be found when a dislocation intersected with the sample surface. With further increase of sample thickness, a clear two-layer structure (a strained defect-free layer and a relaxed layer with high defect density) could be observed. The area close to the interface had almost no defects but above it long stacking faults (several hundred of nanometers) could be observed. These stacking faults were stacked on top of each other and the vertical separation measured was about 10 nm-30 nm. The surface of the sample had a saw-like shape with a roughness (measured from the valley to the top) of more than 100 nm. In this sample some small randomly distributed domains were formed with closely separated planar defects.

An increase of the layer thickness led to a higher density of long planar defects and the number of domains also increased together with their size (Fig. 2b, marked by arrows). It was interesting to note that these domains were surrounded by voids. High-resolution electron microscopy and Z-contrast microscopy using High Angle Annular Dark Field (HADDF) revealed the formation of basal stacking faults [15] with large areas of cubic material, larger than expected for a particular type of stacking fault in the wurtzite structure. There are areas in the sample where cubic material can remain to the top of the layer surface, but in the majority cases these “polytype-like areas” can be converted back to a hexagonal layer arrangement with a high density of randomly distributed stacking faults. More details on this subject have been reported earlier [15]. For the sample with the larger thickness of 730 nm, some planar defects and domains with “polytype-like arrangement were “pushed” to the interface and such a layer was almost completely relaxed.

3.3 X-ray studies Two methods were applied to all five samples: high resolution X-ray diffraction (HRXRD) by collecting 2θ/ω scans and reciprocal space maps. HRXRD studies showed a single peak for the thinnest sample that was slightly shifted toward the GaN peak for the 200 nm thick sample. Already for the 400 nm thick sample, where the formation of long stacking faults was observed by TEM, a second peak could be observed even closer to the GaN peak [15]. With an increased layer thickness this second peak shifted closer to the GaN peak and

Table 1 Lattice parameters and In content (X-ray studies).

Samples	c (Å)	a (Å)	c_{relax} (Å)	a_{relax} (Å)	x (%)
GaN exp	5.1886	3.1866			
S196-100 nm strained	5.25248	3.1841	5.2228	3.2417	7.3
S192-250 nm strained relaxed	5.2474 5.2474	3.1841 3.2175	5.2221 5.2393	3.2143 3.2259	7.2 10.5
S004-500 nm strained relaxed	5.2458 5.2243	3.1950 3.2200	5.2251 5.2268	3.2163 3.2174	7.8 9.4
S005-750 nm strained relaxed	5.2527 5.2331	3.1887 3.2229	5.2256 5.2338	3.2166 3.2222	7.8 9.4

© 2009 WILEY-VCH Verlag GmbH & Co. KGaA, Weinheim

had higher intensity. Two clear peaks (or more since the full width at half maximum is rather broad) indicate the presence of two sublayers with two different *c* parameters, where the split of the layer can be related to the onset of relaxation in the InGaN layer or a difference in Indium composition. Assuming the validity of Vegard's law for the lattice parameters and using the elastic constants of InN and GaN [16], the Indium compositions was determined by applying Schuster's equations [17]. Table 1 gives the Indium content and lattice parameters.

X-ray reciprocal maps confirmed TEM observations and showed that the thinnest layer was completely strained. The reciprocal node was arranged in the same line as GaN (Fig. 3a). With an increased layer thickness the second node appeared with increasing intensity. For the largest layer thickness the intensity of the new node dominated leaving only a small indication of the presence of the node from the strained layer (Fig. 3b).

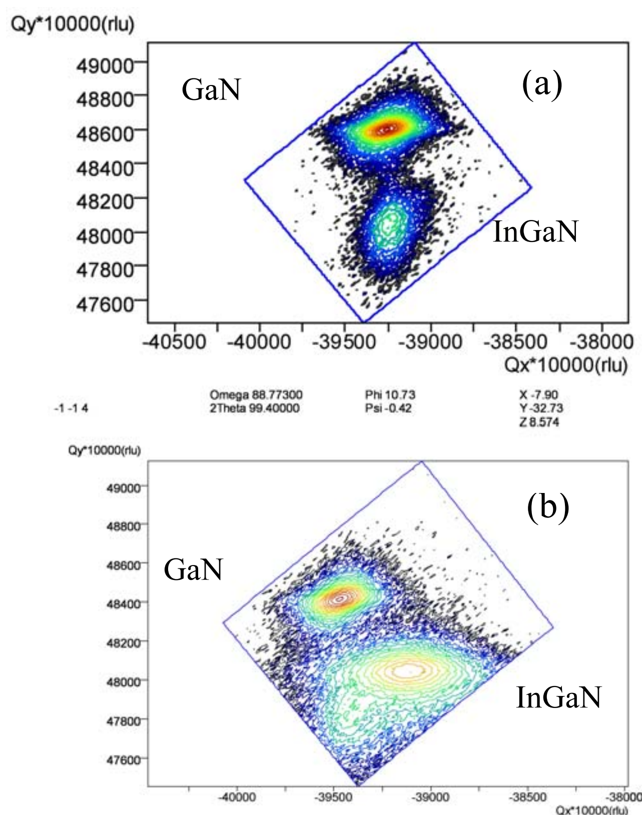

Figure 3 Reciprocal space maps for assymetrical $\bar{1}\bar{1}24$ reflection from the InGaN samples with the nominal thickness of 100 nm (a) and 750 nm (b). Note formation of two nodes: one with lattice parameter as GaN and the second from the relaxed part of the layer.

3.4 RBS studies The RBS spectra were taken from each of five samples and later simulated to determine the layer thickness and a composition. An excellent agreement was obtained for the thinnest sample. The experimental and calculated spectra overlapped (Fig. 4) with an assumption of a layer thickness of 63nm (69 nm from TEM) and a composition of 7% (7.3% ± 0.5% from HRXRD). For the thicker layers there was no agreement when only two compositions (as determined by HRXRD) were taken into account. The full agreement with the experimental curves was obtained only when the relaxed parts of the layers were sequestrated into sub-layers with varying composition as shown in Table 2. It is therefore, expected that the atomic arrangement in the defective parts of the layers might lead to different compositions.

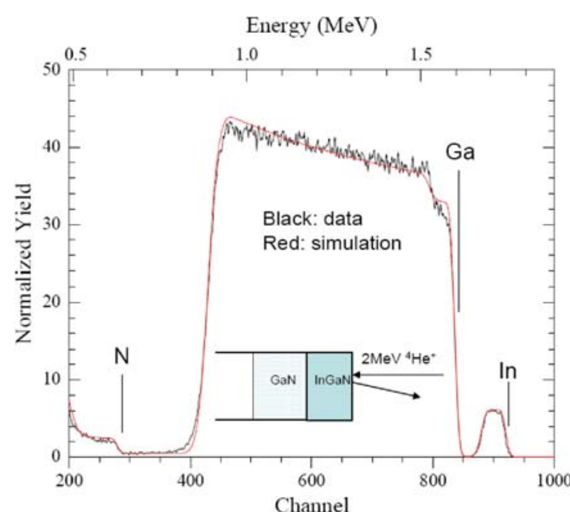

Figure 4 RBS spectrum from the thin sample.

Table 2 Layer thickness in the sublayers estimated based on RBS studies. First column gives the nominal thickness of a whole layer and next columns give the thickness and In content in the sublayers to match the experimental curves. The arrows in the columns indicate sublayer stacking direction till the surface is reached in each sample.

Samples			
S196-100 nm			
t (nm)	63		
x (%)	7		
S192-250 nm			
t (nm)	40→	40→	58→
x (%)	8.5	10.5	11
t (nm)	26 surface		
x (%)	9.9		
S004-750 nm			
t (nm)	52→	92→	92→
x (%)	9	13.5	14
t (nm)	92→	80→	80→
x (%)	13	11.5	10.5
t (nm)	46 surface		
x (%)	9.5		

© 2009 WILEY-VCH Verlag GmbH & Co. KGaA, Weinheim

3.5 Cathodoluminescence (CL) studies It was clear from the TEM studies that the structural quality is changing with layer thickness, therefore, out of the five cross-section samples that were studied earlier by TEM and well characterized, two were chosen for CL studies. We wanted to see how the structural quality of the sample influences the CL peak position. Therefore, the experiment was set on the thinnest sample, where TEM studies indicate as almost defect free sample and the second sample with the measured thickness of 520 nm (nominal 750 nm) where long stacking faults, domains with closely separated planar defects ("polytype-like") and large areas of cubic material were formed. The CL spectra were taken from the different areas of the samples: the Al_2O_3 substrate, the GaN buffer layer and the InGaN layer. CL spectra were then taken by focusing the beam onto a single spot ("spot-mode") at various locations across the cross-section sample (substrate, interfacial area and several spots in the layer). Though the radius of this electron beam spot is very small (~2-5 nm), the volume in the material throughout which electron-hole pairs are generated is much larger and ultimately dictates the spatial resolution our CL measurements. For the thinnest sample CL peaks appear at 2.97 eV from the InGaN layer and 3.296 eV from the GaN, slightly lower than the energy gap of GaN (3.4 eV). Two peaks are also observed from the substrate, one at lower energy (1.6 eV) and one at higher energy of 3.7eV (Fig. 5a).

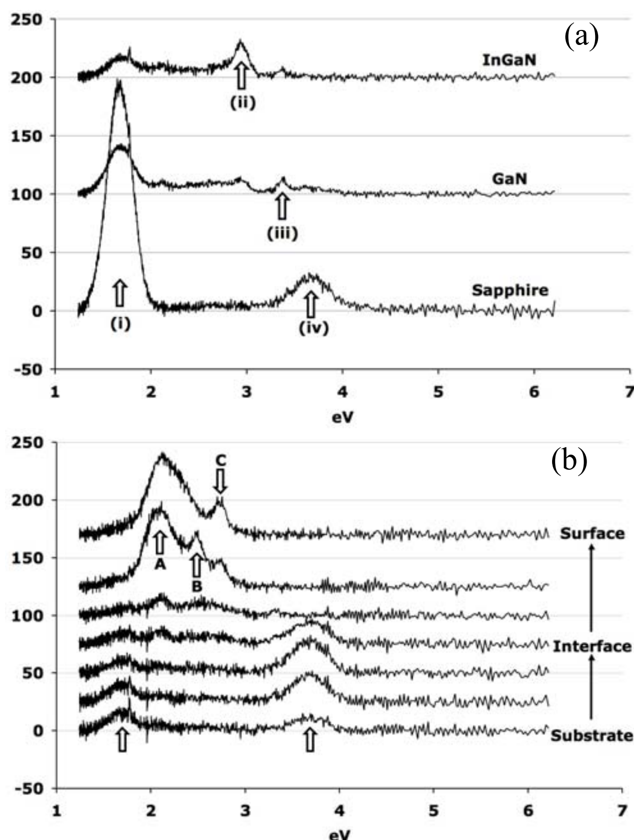

Figure 5 CL spectra from: (a) the thin sample (nominal 100 nm) and (b) from the thick sample (nominal 750 nm). The arrows indicate peaks with different energies: I-1.606eV, II-2.974eV, III-3.296eV; IV-3.64 eV; A-2.076eV, B-2.468eV and C-2736 eV.

For the thicker sample (where the structural perfection varies with sample thickness) several spectra were taken; starting from the substrate, through the interfacial area to the sample surface. One can notice that the peaks for the substrate and GaN remain in the same positions as observed for the thin sample (Fig. 5b). However, at some point indicated on Fig. 5b as "interface" a peak at 2.076 eV (A) appears and remains through the entire layer to the top surface. A second peak at 2.468 eV (B) also starts at the interfacial area with a low intensity, increases intensity in the central part of the layer but then completely disappears at the sample surface. The third peak at 2.736 eV (C) appears only in the central part of the InGaN layer and remains to the top surface. One should notice that there are different peak positions at different parts of the layer and the peak that was observed for the thinnest sample is not observed at any place of the thick sample. A simple calculation of the dependence of the wave length and energy gap on InN fraction in the InGaN is presented by equation below and this dependence is shown on Fig. 6.

$$E_g(x) = E_g(InN)(x) + E_g(GaN)(1-x) - bx(1-x)$$

Here we use the bowing parameter b = 1.43 eV after Wu et al. [18].

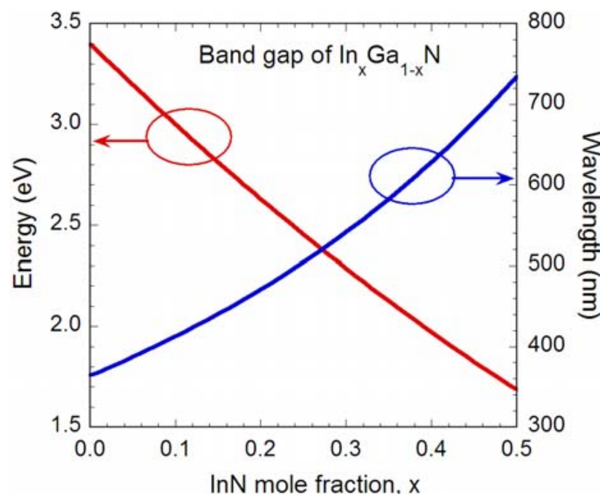

Figure 6 Calculated bangap energies and wavelength for different InN mole fractions.

Based on the dependence shown above one can notice that the energy of 2.97 eV (Fig. 5a - peak II) observed in the thinnest sample would require 10% InN. This is the expected nominal concentration, which was very close to the 7% estimated from both RBS and X-ray studies. However, for the second thick sample the energy of 2.076 eV (Fig. 5b - peak A) would require 40% InN, B-2.468 eV-24% InN and C-2.736-19% InN.

© 2009 WILEY-VCH Verlag GmbH & Co. KGaA, Weinheim

4 Discussion and conclusions This study shows that $In_xGa_{1-x}N$ samples are very complex and the structural quality is changing even for low In contents if larger sample thicknesses are grown. Only for small sample thickness, (not exceeding 70-100 nm) are practically defect free layers observed. This composition is lower than the nominal (confirmed by X-ray studies and RBS) since the strained layer tries to match the underlying GaN and rejects In, most probably to the sample surface, causing an excess of In. With such an In excess, the presence of intrinsic dislocation loops with an inserted layer would be expected, most probably rich in In. Therefore, it is not surprising that as soon as the sample thickness exceeds the critical layer thickness planar defects start to appear. This is in contrast to the assumption of In droplet formation frequently cited in the literature [10-13]. These planar defects in the layers with a thickness of about 200 nm can be better described as intrinsic Frank type dislocation loops, where the inserted layer is a stacking fault. For an increase of sample thickness these stacking faults (loops with a large diameter) become longer and longer, as seen on cross-sectional TEM micrographs, and the vertical separation between them also becomes smaller. There are areas where these planar defects are so close to each other that small domains are formed with almost “polytype-like” arrangement. The presence of small voids in their surrounding areas might suggest local conglomeration of N vacancies to form these voids. The local change in distribution of these planar defects would explain the RBS data suggesting layer sequestration into sublayers with different In concentration. $In_xGa_{1-x}N$ layers start to relax by the formation of planar defects. This is confirmed by the formation of an additional node in the reciprocal mapping. One needs to notice that there are no additional dislocations formed at the interface with GaN. The dislocations that are present in the layer are the same as those that originated at the Al_2O_3 substrate interface.

Only for the thinnest, strained, defect free sample was a single band edge PL peak observed. Samples with larger thicknesses showed multiple peaks corresponding to layers with different In contents. However, much higher In contents than measured would be required to explain the presence of some PL peaks with longer wavelengths. These results would suggest that some PL peaks are coming from defects in the relaxed part of the layers. This was clearly confirmed by CL studies where peaks with different energy (wave length) appear in the thin sample and in the defective sample, where the atomic arrangement is different. These studies clearly show the influence of structural defects on optical properties and we are working on obtaining CL spectra from individual defects to better understand the origin of particular peaks.

Acknowledgements This work is supported by the Director, Office of Science, Office of Basic Energy Sciences, Division of Materials Sciences and Engineering, of the U.S. Department of Energy under Contract No. DE-AC02-05CH11231. CL measurements were performed at the Molecular Foundry, Lawrence Berkeley National Laboratory, also supported by the same Office. The authors are thankful to D. Frank Ogletree and E. K. Wong for experimental assistance with the CL measurement setup." The use of the facility of the National Center for Electron Microscopy in LBNL, Berkeley is appreciated.

References

[1] S. Nakamura and G. Fasol, in: The Blue Laser Diode (Springer, Berlin, 1997).
[2] Y. Narukawa, M. Sano, T. Sakamoto, T. Yamada, and T. Mukai, Phys. Status Solidi A **205**, 1081 (2008).
[3] G. Chen, M. Craven, A. Kim, A. Munkholm, S. Watanabe, M. Camras, W. Götz, and F. Steranka, Phys. Status Solidi A **205**, 1086 (2008).
[4] H. Ho and G. B. Stringfellow, Appl. Phys. Lett. **69**, 2701-27013 (1996).
[5] A. Zunger and S. Mahajan, in: Handbook on Semiconductors, Vol. 3, ed. S. Mahajan (North Holland, Amsterdam, 1994).
[6] N. A. El-Masry, E.I. Piner, S.X. Liu, and S. M. Bedair, Appl. Phys. Lett. **72**, 40 (1998).
[7] Z. Liliental-Weber, M. Benamara, J. Wasahburn, J. Z. Domagala, J. Bak-Misiuk, E. L. Piner, J. C. Roberts, and S. M. Bedair, J. Electron. Mater. **30**, 439 (2001).
[8] S. Pereira, M. R. Correia, E. Pereira, K. P. O'Donnell, E. Alves, A. D. Sequeira, N. Franco, I. M. Watson, and C. J. Deatcher, Appl. Phys. Lett. **80**, 3913 (2002).
[9] S. Pereira, M. R. Correia, T. Monteiro, E. Pereira, E. Alves, A. D. Sequeira, and N. Franco, Appl. Phys. Lett. **81**, 1207 (2002).
[10] S. Chichibu, T. Azuhata, T. Sota, and S. Nakamura, Appl. Phys. Lett. **69**, 4188 (1996).
[11] D. M. Graham, A. Soltani-Vala, P. Davson, M. J. Godfrey, T. M. Smeeton, J. S. Barnard, M. J. Kappers, C. J. Humphreys, and E. J. Thrush, J. Appl. Phys. **97**, 103508 (2005).
[12] Y. Narukawa, Y. Kawakami, M. Funato, S. Fujita, and S. Nakamura, Appl. Phys. Lett. **70**, 981 (1997).
[13] H. K. Cho, J. Y. Lee, N. Sharma, C. J. Humphreys, G. N. Yang, C. S. Kim, J. H. Song, and P. W. Yu, Appl. Phys. Lett. **79**, 2594 (2001).
[14] C. J. Humphreys, M. J. Galttrey, N. Van der Laak, R. A. Oliver, M. J. Kappers, J. S. Barnard, D. M. Graham, and P. Dawson, in: Microscopy of Semiconducting Materials, eds. A. G. Cullis and P.A. Midgley (2007), p. 3.
[15] Z. Liliental-Weber, K. M. Yu, M. Hawkridge, S. Bedair, A. E. Berman, A. Emara, J. Domagala, and J. Bak-Misiuk, Phys. Status Solidi C **6**, S433 (2009).
[16] J. H. Edgar et al. (ed.), Properties, Processing and Applications of GaN and Related Semiconductors (London: Data rev. Ser. No. 23, 1999).
[17] M. Schuster, P.O. Gervais, B. Jobs, M. Hosler, R. Averbeck, M. Riechert, A. Iberl, and M. Stommer, J. Phys. D: Appl. Phys. **32**, A56 (1999).
[18] J. Wu, W. Walukiewicz, K. M. Yu, J. W. Ager III, E. E. Haller, Hai Lu, and W. J. Schaff, Appl. Phys. Lett. **80**, 4741 (2002).

© 2009 WILEY-VCH Verlag GmbH & Co. KGaA, Weinheim